



# Design Studies of Large Aperture, High-Resolution Earth Science Microwave Radiometers Compatible With Small Launch Vehicles

---

*Lyle C. Schroeder, M. C. Bailey, Richard F. Harrington, Bruce M. Kendall, and Thomas G. Campbell*



# Design Studies of Large Aperture, High-Resolution Earth Science Microwave Radiometers Compatible With Small Launch Vehicles

---

*Lyle C. Schroeder and M. C. Bailey*  
*Langley Research Center • Hampton, Virginia*

*Richard F. Harrington*  
*Old Dominion University • Norfolk, Virginia*

*Bruce M. Kendall and Thomas G. Campbell*  
*Langley Research Center • Hampton, Virginia*

#### Acknowledgment

The authors gratefully acknowledge the help provided by Washita Sasamoto for orbital analysis, David Butler for payload system packaging studies, and Roland Lawrence for consultative support on radiometer system design.

This publication is available from the following sources:

NASA Center for AeroSpace Information  
800 Elkridge Landing Road  
Linthicum Heights, MD 21090-2934  
(301) 621-0390

National Technical Information Service (NTIS)  
5285 Port Royal Road  
Springfield, VA 22161-2171  
(703) 487-4650

## Symbols and Abbreviations

AMSR	Advanced Microwave Scanning Radiometer
A/D	analog to digital (fig. 9)
BPF	band pass filter (fig. 9)
CMOS VLSI	complimentary metal oxide semiconductor very large scale integration
$D$	reflector aperture height (fig. 8)
DMSP	Defense Meteorological Satellite Program
EOS/MLS	Earth Observing System/Microwave Limb Sounder
ERS-1	European Remote Sensing Satellite 1
ESA	European Space Agency
ESTAR	Electrically Scanned Thinned Array Radiometer
$F$	focal length (fig. 8)
GFSC	Goddard Space Flight Center
H	horizontal (polarization) (fig. 10)
HARD	High Accuracy Reflector Development
IAE	Inflatable Antenna Experiment
JPL	Jet Propulsion Laboratory
LNA	low noise amplifier (fig. 9)
MIMR	Multifrequency Imaging Microwave Radiometer
MMIC	microwave monolithic integrated circuit
MUX	multiplexer (fig. 9)
PBMR	pushbroom microwave radiometer
PIN	positive intrinsic negative (p-material, intrinsic, n-material)
pol	polarization
$R$	displacement from axis of rotation (fig. 8)
RF	radio frequency
rms	root mean square
RTD	resistance temperature device (fig. 9)
SLD	square law detector (fig. 9)
SSM/I	Special Sensor Microwave/Imager
SSMIS	Special Sensor Microwave Imager Sounder
S/H	sample/hold (fig. 9)
SW	switch (fig. 10)
$T$	temperature (microwave radiometer measurement)
TMI	TRMM Microwave Imager
TRMM	Tropical Rain Mapping Mission
V	vertical (polarization) (fig. 10)

Subscripts:

ant	antenna
inj	injection
ref	reference
sys	system

## Summary

The Langley Research Center has been investigating the critical technologies for developing advanced real aperture microwave radiometers suitable for Earth science observations. A significant objective of this research is to enable microwave measurements with adequate spatial resolutions for a number of Earth science parameters, such as sea ice, precipitation, soil moisture, sea surface temperature, and wind speed over oceans. High-spatial-resolution microwave radiometer sensing from space with reasonable swath widths and revisit times favor large aperture systems. However, with traditional precision antenna design, the size requirements for such systems are in conflict with the need to emphasize small launch vehicles. For example, K-band observations of sea ice requires an antenna of approximately 4 m in diameter and antennas in the 20 to 30 m category will be needed for L-band measurements of soil moisture in order to satisfy science requirements for a resolution of 10 km from low Earth orbit. This paper describes trade-offs between the science requirements, basic operational parameters, and expected sensor performance for selected satellite radiometer concepts. The preliminary designs of real aperture systems utilizing novel lightweight compact-packaging techniques are used as a means of demonstrating this technology. Radiometer subsystem design and calibration as well as antenna and feed design criteria and techniques required are also presented. Preliminary results show that novel designs and packaging techniques compatible with small launch systems coupled with state-of-the-art radiometer designs hold promise for high-resolution Earth science measurement systems.

## 1. Introduction

Current operational technology is unable to fulfill key science needs in remote sensing from space. For example, microwave measurements of sea ice, soil moisture, salinity, and wind speed are not being obtained at the required spatial Earth resolution. The Low Earth Orbit Microwave Radiometry Workshop held in Hampton, Virginia, September 22–24, 1992, identified measurements of soil moisture at a resolution of 10 km as the general science driver. Likewise, measurements of salinity and sea ice are significantly short of the mark for science needs. Sensing of wind speed by the Seasat and ERS-1 scatterometers has been confined to resolutions from 25 to 50 km.

Higher spatial resolution can be achieved traditionally by providing larger real apertures or by the application of synthetic aperture (thinned array) techniques. Thinned arrays remove much of the

bulk of the antenna by using elements at carefully selected positions (related to a wavelength) and “filling in the antenna pattern” with computer processing techniques. They are attractive for single frequency remote-sensing applications, such as soil moisture, but increase in complexity with added frequencies and polarizations. Researchers at the Goddard Space Flight Center (GSFC), the Jet Propulsion Laboratory (JPL), and the University of Massachusetts have proposed using this concept in one- and two-dimensional synthetic aperture systems such as the Electronically Scanned Thinned Array Radiometer (ESTAR). (See ref. 1.) A recent study at the Langley Research Center of a 1.4-GHz two-dimensional ESTAR soil moisture radiometer required 20 880 correlators and had a data rate of 448 kbps. The power consumption was estimated at 0.62 mW/correlator. The 1992 state-of-the-art correlators using advanced custom designed CMOS VLSI technology, developed by JPL for the EOS/MLS project, consume 47 mW/correlator (ref. 2), almost 2 orders of magnitude higher. The weight of the correlators requires similar improvement. Thus, the success of these systems seems to depend on future significant breakthroughs in the development of low-power and low-weight correlators and receivers.

The radiometer technology that is employed in real aperture pushbroom radiometer systems utilizes significantly less complex electronic circuitry as compared with the electronic subsystems required for synthetic aperture radiometers. Traditional real aperture system design utilizes a more mature technology. The Langley Research Center and other NASA centers have designed radiometers utilizing this technology since well before 1970. Pushbroom concepts have been developed which allow multiple simultaneous beams without electronic or mechanical scanning (ref. 3). Real aperture reflector antenna systems can be used for simultaneous multiple frequencies provided the surface size and roughness criteria are met for both the upper and lower frequencies. Radiometers can use direct detection receivers, which allow simpler and less expensive systems. Historically large antennas have not been employed in many space applications because of the substantial penalty in associated physical weight and packaging volume required. To illustrate this point, the resolution provided by relevant operational and planned remote-sensing radiometers is summarized in figure 1. The minimum antenna diameter required to achieve resolutions from 25 to 1 km from an orbit of 400 km at an incidence angle of  $50^\circ$  is plotted as a function of frequency. The frequencies used to detect salinity and soil moisture, sea surface temperature,

ocean wind speed, and sea ice are shown in this plot. The antenna diameters are noted for the operational Special Sensor Microwave/Imager (SSM/I) (ref. 4), ESA Multifrequency Imaging Microwave Radiometer (MIMR) (ref. 5), Advanced Microwave Scanning Radiometer (AMSR) (ref. 6), and the Tropical Rain Mapping Mission (TRMM) Microwave Imager (TMI) (ref. 7). The TMI uses the same antennas as the SSM/I. These missions all use mechanically scanned radiometer reflectors, which limits the maximum diameter, and hence, the resolution achievable. From this figure, a soil moisture measurement at 1.4 GHz and a resolution of 10 km from an altitude of 400 km would require an antenna 45 times larger than the SSM/I antenna. (See fig. 1.) Previous studies of precision deployable, large aperture systems yielded antennas with high areal density (5–10 kg/m<sup>2</sup>) which require significant portions of a shuttle bay to launch (ref. 8). These results are clearly not in accord with present emphasis on low-cost payloads suitable for small expendable launch systems.

Recently, new novel designs for lightweight reflector systems have been developed by private industry and have been studied for their application to microwave radiometer remote-sensing systems. One such system, the high accuracy reflector development (HARD) system developed by TRW, Inc., consists of hexagonal segments deployed and latched together by novel rotational/translational joints. TRW has built a 5-m-diameter deployable ground test model of this antenna with an overall surface accuracy of better than 0.23 mm (0.009 in.) rms. (See fig. 2.) Lightweight graphite-epoxy panels approximately 0.25 mm thick are supported at the edge by hexagonal hoops made of graphite-epoxy tubes approximately 2.5 cm in diameter. The prototype consisted of seven hexagonal panels approximately 1.75 m across. (See ref. 9.) The stowed antenna occupied a volume 0.6 m high by 2 m in diameter. Deployment was achieved by novel joints at one apex of each panel which rotated the stack of panels into each panel position and latched the bottom panel into position. The prototype antenna was successfully tested at TRW for acoustics, vibration, deployment accuracy, and near-field antenna patterns at 60 GHz (results available upon request). The entire assembly weighed less than 40 kg and overall surface roughness was less than 0.23 mm (0.009 in.) rms. Preliminary results with advanced panels at TRW indicate that additional significant improvement in surface accuracy can be achieved with a thin lightweight solid panel reflector.

A second system is a deployable inflatable structure to which a thin reflective layer is deposited to

form a reflector, which is joined to a feed system and spacecraft bus. (See fig. 3.) A 14.7-m model using this system is being developed under the In-Space Technology Experiment Program (IN-STEP) (refs. 10 and 11) by L'Garde, Inc., and managed by JPL. This IN-STEP program will determine the reflector surface accuracy possible by using this antenna concept in a space environment.

System studies of the application of these real aperture antenna radiometer systems to Earth remote-sensing missions is the subject of this paper. The HARD system concept was applied to an ice and precipitation imaging mission at 18.7 and 36.5 GHz, where reflector surface precision requirements are more stringent. The inflatable system is being applied to a soil moisture (1.4-GHz) mission where tolerances are greater. Companion sensors utilizing the inflatable reflector measure sea surface temperature (at 4.3 GHz), and wind speed (at 10.65 GHz). Resulting system size, performance, and an assessment of the feasibility are discussed.

## 2. Real Aperture Technology

The conical pushbroom concept, illustrated in figure 4, provides high-resolution contiguous measurements as simultaneous beams move across the Earth's surface to cover a specified swath width. The illustration in figure 4 is not drawn to scale. The conical pushbroom satellite instrument in low Earth orbit would produce simultaneous circular footprints (–3-dB beam contours) at a beam incidence angle of 53° with respect to the surface normal of the spherical Earth. The simultaneous beams are produced in a circular arc in order to maintain the same incidence angle for all beams. By maintaining the same incidence angle, the software algorithms for inversion of measured data are the same for each beam. Each beam consists of dual orthogonal parallel and perpendicular polarizations with respect to the plane of incidence. The circular footprints are achieved by producing an elliptical beam from the antenna such that its intersection with the surface of the Earth forms a circle. The swath width is determined by the size and number of simultaneous beams. The staggering of the beam footprints, shown in figure 4, is a result of the antenna feed panel layout, as described subsequently.

The antenna concept is shown in figure 5. It consists of an offset parabolic torus reflector with multiple feeds on a circular arc. The feed panel is illustrated in figure 6 and consists of individual planar arrays of dual-polarized microstrip patch radiators. Each feed array is designed for proper illumination of a portion of the parabolic torus in order to produce

the desired elliptical beam. Low sidelobes and low spillover are required in order to achieve main beam efficiency of 90 percent or greater. A reflector edge illumination taper of  $-15$  dB was chosen in order to produce the required low sidelobes. In addition, the feed array is designed with a tapered excitation in order to reduce the feed array pattern sidelobes, with a corresponding reduction in the reflector spillover loss. With the feeds located in a row along a circular arc, the corresponding beams from the parabolic torus are separated by two beamwidths; therefore, a second row of feeds are located along a slightly displaced arc and shifted, in order to produce beams which fill in the spaces between the previous arc of beams. Because the two rows of feeds are on opposite sides of the focal arc, a staggered arrangement of footprints, as shown in figure 4, are produced. The feed panel in figure 6 is for a single frequency. For radiometer instruments requiring multiple frequencies, additional rows of feeds can be added. A portion of a feed panel layout for a three-frequency system, to be discussed later, is illustrated in figure 7.

The parabolic torus reflector surface in figure 5 is obtained by rotation of an offset portion of a parabola about a tilted axis. This geometry is illustrated in figure 8. The required angle of tilt  $\alpha$  is determined by a combination of the orbit altitude and the required beam incidence angle at the surface of the spherical Earth. For an incidence angle of  $53^\circ$  and an altitude of 400 km, the tilt angle is  $48.7^\circ$ . The displacement  $R$  from the axis of rotation is specified for optimum torus design. An approximate value for  $R$  can be obtained from  $F/(F + R) = 0.487$  (ref. 12), where  $F$  is the focal length of the parabola. The amount of angular rotation of the parabola is dictated by the desired swath width and, therefore, establishes the total width of the reflector in that direction and the arc length of the feed panel. The reflector aperture height  $D$  determines the antenna beamwidth in the plane of incidence, and its specific size is a function of the altitude, beam incidence angle, and footprint size for a specific frequency. The ratio of focal length to aperture height  $F/D$  is selected as 1.5 in order to reduce the reflector cross-polarization to an acceptable level (i.e.,  $-35$  dB or lower). A broader beamwidth orthogonal to the plane of incidence is necessary in order to produce a circular footprint on the Earth's surface; therefore, the effective illumination width of the reflector in that direction will be less than  $D$ . For an altitude of 400 km and incidence angle of  $53^\circ$ , the ratio of the beamwidths (and inversely the ratio of reflector aperture illumination widths) is 1.65.

Each array feed illustrated in figures 6 and 7 is intended to be somewhat generic in the sense that it

represents a dual-polarized planar array with the desired radiation characteristics for illumination of the reflector at a specified frequency. Although an array of series-fed square microstrip patches could provide the desired illumination with simultaneous vertical and horizontal polarization while occupying a minimal volume, the specific detailed design has not been completed. Such specifics as the sizing of individual patches for proper excitation, array element mutual interactions, feed line radiation, cross coupling between orthogonal polarizations require further study. The simplicity and minimal packaging volume of the single board configuration in figure 7 appears promising and warrants a more detailed design evaluation. Should this configuration prove to lack the capability of meeting requirements, multiple board configurations which utilize corporate feed networks with feed-through connections would offer alternative solutions with their additional inherent complexities, losses, and increased volume and weight.

### 3. Radiometer Technology

The radiometer technology employed in existing spaceborne systems uses real aperture antenna technology. The existing and planned spaceborne radiometer systems are mechanically scanned systems. The highly successful spaceborne radiometer, the Special Sensor Microwave/Imaging (SSM/I) for the Defense Meteorological Satellite Program (DMSP), is a mechanically scanned total power radiometer. The entire radiometer including the reflector, antenna feeds, and radiometer electronics are mechanically rotated at a constant rate of 30 rpm. The radiometer scans the measurement scene approximately  $140^\circ$  out of the  $360^\circ$  of one revolution; during the other  $220^\circ$ , the radiometer scans a hot target and a cold sky target for calibration purposes. For this scenario, the radiometer is calibrated every 2 sec. The frequent calibrations allow the use of total power radiometers for these systems, which offer the best radiometric sensitivity for a given bandwidth and integration time.

The reflector sizes for mechanically scanned radiometers are limited to approximately 2 m for several reasons. First, an increase in the antenna size results in a corresponding decrease in the resolution cell size. Since the satellite downlink velocity is constant, the rotational velocity must be increased to satisfy Nyquist sampling requirements in this dimension. Multiple beams downtrack could be used to satisfy this requirement but would increase the radiometer complexity and cost. A second reason is the requirement for momentum compensation to keep the platform stable. The antenna diameter is a



control system driver; if either the rotating radiometer or the momentum compensation wheel should fail, the spacecraft control system must prevent the spacecraft from spinning out of control while the other device is powered down. The third reason is the complexity of fitting an antenna larger than 2 m in diameter inside a shroud of a launch vehicle and deploying it into proper configuration and position for mechanically scanning the Earth's surface.

Future space missions plan to employ total power radiometer with direct detection and mechanically scanning real aperture antenna systems. SSMIS on future DMSP satellites, TMI on the Tropical Rain Mapping Mission (TRMM), the ESA Multifrequency Imaging Microwave Radiometer (MIMR), and the Japanese Advanced Mechanically Scanned Radiometer (AMSR) all employ this radiometer technology.

An alternative solution to the problem of obtaining high spatial resolution without any mechanical scanning is a pushbroom radiometer system. The pushbroom technique utilizes simultaneous measurements by fixed scanned multiple beams. The radiometer is constantly observing the scene; therefore, providing time for calibrations without mechanically moving either the antenna or the feed to the calibration target is a significant problem. Frequent calibrations are required because of the gain instabilities of the radiometer receivers operating in a total power mode. A radiometer technique employed successfully in many airborne remote-sensing applications is that of balanced Dicke noise injection. The gain instability problem is eliminated with classical feedback techniques at a penalty of degrading the sensitivity by a factor of 2 over that of an ideal radiometer.

The effect of short-term gain variations is eliminated in a balanced Dicke radiometer because the signal (noise) levels when the radiometer is measuring the antenna port and the reference load are identical. This balanced condition in the Dicke radiometer is achieved by adding noise from an avalanche noise diode  $T_{inj}$  to the received radiometric antenna temperature  $T_{ant}$ . This sum is added to the radiometer receiver system noise temperature  $T_{sys}$  during one half of the Dicke cycle. The avalanche noise diode is operating at a constant power level and physical temperature. The injected noise is controlled by a PIN diode switch which injects a known noise level. During the other half of the Dicke cycle, the radiometer measures the noise from a precision load resistance which is maintained at a constant and accurately known physical temperature  $T_{ref}$  ( $\pm 0.05^\circ\text{C}$ ). A first-order, closed-loop feedback circuit with zero position error accurately adjusts the amount of injected noise such that  $T_{inj} + T_{ant} = T_{ref}$ . The accuracy of

a noise injection radiometer and the resultant calibration requirements are a function of the stability of the output power from the avalanche noise diode with temporal and physical temperature variations. Available test data (ref. 13) show temporal variations of  $\pm 0.01$  percent/hour and  $\pm 0.1$  percent/day or  $\pm 0.03$  K/hour and  $\pm 0.3$  K/day, respectively, for an injected noise level of 300 K. The variation with physical temperature is 0.2 percent/ $^\circ\text{C}$ , which is 0.6 K/ $^\circ\text{C}$ . Physical temperature measurements of the avalanche noise diode can be accomplished with an accuracy of  $\pm 0.05^\circ\text{C}$ .

A real aperture pushbroom radiometer using a noise injection balanced Dicke radiometer would require calibration at an interval from once per orbit to once per day. Several schemes proposed to achieve this calibration include interval calibration using a cooled and a heated resistive load for the cold and hot calibration points, respectively; moving a calibration load in front of the feeds by mechanical means; measuring known Earth scenes; or observing cold sky by rotating the spacecraft to deep space once per calibration period.

A radiometer system design, based on the real aperture pushbroom radiometer concept, has been developed by the Langley Research Center to provide high-resolution radiometric measurements of geophysical parameters from low Earth orbit. The basic design of the radiometer receiver is shown in figure 9. Recent advances in square law detectors have enabled the use of direct detection at frequencies greater than 50 GHz while still achieving the stringent detector linearity requirement for a precision radiometric measurement. Direct detection allows the elimination of the local oscillator and mixer and significantly reduces power consumption. With MMIC and other advanced technologies, receivers can be designed which weigh between 2 to 2.5 lb and consume only a few watts of power.

An additional advantage in the application of pushbroom technology is that one receiver can be electronically time-multiplexed between several beams and have sufficient integration time per beam to meet the radiometric sensitivity requirements. Figure 10 shows a radiometer assembly in which eight beams are multiplexed to one radiometer receiver. The injected noise must be injected at the feeds of the radiometric antenna, this is accomplished by using the noise module shown in figure 11. The power output from one avalanche noise diode is sufficient for feeding 16 radiometer channels. The noise source module for the design shown in figure 12 feeds eight noise modules. Each noise module simultaneously feeds a separate vertical and horizontal polarization

multiplexer system. (See fig. 10.) With this design, the vertical and horizontal radiation from each resolution cell can be measured simultaneously.

In order to test the performance capabilities and the component requirements for such a spaceborne system, a precision radiometric measurement laboratory is under development at the Langley Research Center and will be operational in 1994. A radiometer with a frequency of 4.3 GHz and using digital signal processing is under construction; this radiometer will be capable of operating in a total power mode, an unbalanced Dicke mode, and a balanced Dicke mode. Precise physical temperature measurements along with statistical data analysis techniques provide the capability to obtain needed data on gain instabilities of low noise amplifiers, system noise temperature variations within radiometer components, and capabilities of new calibration techniques. One of the first projects for this laboratory is the extensive evaluation of the stability with time and temperature of avalanche noise diodes. This information is needed in the design of calibration systems not only for noise injection radiometers but also for correlation radiometers used in synthetic aperture radiometers and scatterometers.

#### 4. System Development Studies

Abbreviated studies have been conducted at Langley to evaluate the requirements for remote-sensing radiometer systems employing recently developed lightweight, large real aperture antenna technology. For the first study, an ice and precipitation imager/mapping system was conceived using the TRW HARD reflector at 18.7 and 36.5 GHz; at these frequencies, the solid reflector panels were believed to be more suited to the reflector surface precision requirements. This study was based to some extent on a design task performed by TRW to extend the design technology from a 7-facet system to an irregular parabolic torus.

The second study used the L'Garde inflatable antenna with a radiometer designed to sense soil moisture (1.4 GHz), where surface precision tolerances were less stringent than for ice. Companion radiometer sensors for this mission were designed for sea surface temperature (4.3 GHz) and ocean wind speed (10.67 GHz).

The objective of the studies was to quantify the weight and packaging requirements to sufficient depth to determine if the mission is compatible with a lightweight launch vehicle. Some attention to cost was also given to scope whether the system cost is within the target maximum system cost including launch vehicle of \$100 million.

##### 4.1. Ice Imaging Radiometer System—Precision Panel Antenna

To demonstrate the applicability of the real aperture technology to space-based radiometer systems, a design study was performed for an ice and precipitation imaging radiometer. The ice-sensing radiometer uses frequencies of 18.7 and 36.5 GHz and requires a reflector whose surface tolerance is 0.165 mm or better (using  $\lambda/50$  as the criteria (ref. 14)).

The system goals for this study were sea ice and precipitation measurements with a spatial resolution of 5 km at 18.7 GHz and 2.5 km at 36.5 GHz. The spacecraft altitude was chosen to be 400 km, the lowest possible with a revisit time less than 5 days and without constant reboost. A conical arrangement of beams at an incidence angle of  $53^\circ$  (selected by the SSM/I science team to optimize the measurement capability) with both horizontal and vertical polarizations was chosen to enhance the scientific return. The antenna beam efficiency was specified as better than 95 percent and the radiometric accuracy to be 1 K. With the methods described in section 2, a 4.3- by 8.2-m parabolic torus antenna, using the HARD technology, was designed to provide contiguous pushbroom radiometer beams along a swath width of 200 km. (See fig. 13.) A printed circuit feed panel, as previously described in section 2, produces 40 beams across track at 18.7 GHz and 80 beams at 36.5 GHz, both with dual polarization. The pushbroom radiometer system uses the time-multiplexed noise injection balanced Dicke radiometer described previously in section 3. Eight beams are time-multiplexed into one radiometer receiver. This requires 10 18.7-GHz radiometers and 20 36.5-GHz radiometers.

The spacecraft packaging is shown in the top left image in figure 14, which is shown in enlarged size in figure 15. A Taurus launch vehicle made by Orbital Sciences Corporation (ref. 15) was found to have adequate capability with margin to launch the instrument, a bus, solar panels, and reboost fuel. The stowed reflector occupies a volume 1.37 m in diameter by 1.07 m high. The TRW Lightsat Eagle bus (ref. 16) is adequate to provide the necessary onboard power and data services for the radiometer/data system. The rest of the deployment scenario for the system is shown in figure 14. On orbit, the main reflector is extended on a boom along with the stack of hexagonal panels. The complete stack of panels is rotated into position and the lowest panel is then translated down and latched into its place on the reflector surface. The panels are deployed in the sequence identified by the numbers on the panels. The feed boom and elements are deployed.

Finally, communications antennas and solar panels (not shown) are deployed. The final (top left) image in figure 14 shows the fully deployed spacecraft. Weights for the instrument, feed, and booms are estimated to be 220 kg; the Taurus system launch capability (635 kg at 400 km) has an adequate margin for the 114-kg Eagle-class bus, solar panels, and reboost fuel. (See table I.) The power requirements are estimated to be 275 W. Table I shows summaries of the characteristics of the system.

The revisit time and the expected lifetime of the sensor satellite were calculated for this system by the Former Space Station Freedom Office at the Langley Research Center. The analyses were based on the fully deployed configuration of figure 14, orbital altitude of 400 km, and a sun synchronous orbit with an inclination of 97.07°. Because the objective of the sensor was to measure ice, the coverage above 50° latitude was sought. The calculated measurement coverage for a revisit time of 3.54 days, shown in figure 16, shows small gaps between swaths. These gaps could be filled in completely in 6.48 days.

The lifetime of the satellite in orbit was calculated for the design configuration. All masses were multiplied by 1.25 in anticipation of future payload growth. Results of these calculations (fig. 17) show a lifetime of less than 100 days at an altitude of 400 km. The mission can be extended significantly by increasing orbit altitudes and scheduling the mission for minimum solar activity. Further increases in lifetime require a trade-off of on-orbit attitude, which can affect swath width, cell size, data reduction algorithms, and other parameters.

In summary, there are some significant design aspects which need further study. First, orbit height versus system drag/reboost fuel needs to be traded off with the aperture size and resolution obtained. Also, the adequacy of the structure to successfully deploy and achieve surface tolerances necessary in orbit needs to be verified, possibly in an IN-STEP experiment. With these qualifications, this preliminary study indicates this system has considerable promise as a low-cost, lightweight remote sensor from space.

#### **4.2. Soil Moisture Radiometer System—Inflatable Antenna**

A design study similar to that conducted for the ice mapping mission is currently being pursued which capitalizes on two important technology programs which were sponsored by the NASA Office of Advanced Concepts and Technology (OACT); that is, the technology development of multiple beam microwave radiometers and the ongoing IN-STEP inflatable antenna experiment (IAE) (See ref. 11.) The

system goals and preliminary weight and power estimates for this study are shown in table II. This system would support the measurement from space of soil moisture, sea surface temperature, and wind speed using the pushbroom concept illustrated in figure 4.

The inflatable antenna concept study includes multiple (pushbroom) beam radiometer sensors, an inflatable reflector to achieve high spatial resolution, and a carrier spacecraft. (See fig. 5.) A small carrier spacecraft is being studied to house the radiometer electronics and multiple beam feed system and provide the container and inflation system for the deployable reflector.

The deployment scenario, as shown in figure 18 for the inflatable antenna radiometer, starts with the packaging of the 1.4-, 4.3-, and 10.65-GHz radiometers; multiple beam feed system; and reflector into a suitable carrier. Once in low Earth orbit at an altitude of 400 km, the carrier is deployed. A start command initiates opening of panels which allows the deployment and inflation of struts and reflector. The inflation system provides nitrogen gas to the struts, torus, and reflector canopy, which comprise the structural elements of the reflector system. After the reflector has been deployed, an inflatable strut will enable the deployment of the phased array feed system for the reflector. Latches located on the ends of the array feed panels will engage at the end of the deployment sequence; therefore, the feed positions are rigidized with the carrier package. The struts attached to the carrier and the reflector will maintain the proper location of the feed system in the focal region of the reflector.

The primary subsystems that comprise the radiometer system include the pushbroom microwave radiometer (PBMR) sensor, the array feed, the inflatable reflector, and the inflation and control subsystem. The PBMR will operate at 1.413, 4.3, and 10.65 GHz with conical multiple beams at an incidence angle of 53°, with measurements at both horizontal and vertical polarizations. The feed array subsystem will consist of microstrip printed circuit elements on low dielectric constant, lightweight foam substrates. (See fig. 7.) The inflatable reflector consists of a 27- by 36-m offset parabolic torus, as described previously in the real aperture technology section. The inflation and control subsystem is based on an extension of the IAE design with modifications due to the structural design changes such as strut lengths and the offset parabolic torus reflector. The inflatable structure, inflation system, and canister would borrow heavily from the technological inheritance from the ongoing IAE. The torus and

struts will be pressurized to about 7000 Pa (1 psi). The inflation system will be housed in a canister similar to the IAE system.

If the surface accuracy demonstration in the IAE proves successful, significant issues will need to be addressed. These include the required thickness (in skin depths) of the metallized reflector surface in order to meet the required low loss performance at 1.4 GHz, the amount of drag in orbit incurred by such a large antenna and its effect on orbital lifetime and required reboost capability, and the on-orbit pointing accuracy and stability of the antenna/feed system.

## 5. Concluding Remarks

The present studies indicate that, by utilizing two novel techniques to obtain a large spaceborne real aperture reflector, pushbroom radiometer systems can be developed that provide passive microwave remote sensing at spatial resolutions of 1 to 10 km of soil moisture, sea surface temperature, ocean winds, sea ice, and precipitation from space. These systems could be launched with small or medium expendable launch vehicles, such as a Taurus or a Titan II. While no detailed analyses of costs were made, the systems considered herein are believed to be on the order of \$100 million or less. The HARD reflector with its precision panels and deployment systems

will most likely be considerably more expensive than the inflatable reflector. The radiometer systems and feeds essentially use the same technology.

The technology required to design and fabricate a spaceborne radiometer sensor for these missions is readily available. The lightweight real aperture reflector technology is much newer, and developments so far are encouraging. The HARD technology has been fabricated and ground based testing has demonstrated this technology. In-space verification of reflector surface accuracy would be a good candidate for a HARD IN-STEP experiment. The ongoing IAE IN-STEP experiment consists of the deployment and surface accuracy measurement of an inflatable antenna during a shuttle mission. Additional trade studies are needed to optimize spacecraft altitude/reboost fuel requirements versus reflector size and its associated Earth resolution cell prior to a radiometer flight experiment. Other major investigations required are the performance of materials for use as radiometer antenna reflectors and the research on stability of avalanche noise diodes, both of which are underway at the Langley Research Center.

NASA Langley Research Center  
Hampton, VA 23681-0001  
August 8, 1994

## References

1. Le Vine, David M.; Wilheit, Thomas T., Jr.; Murphy, Robert E.; and Swift, Calvin T.: A Multifrequency Microwave Radiometer of the Future. *IEEE Trans. Geosc. & Remote Sensing*, vol. 27, no. 2, Mar. 1989, pp. 193–199.
2. Chandra, Kumar M.; Wilson, William J.; and Canaris, John: *Low Power CMOS Digital Autocorrelator Spectrometer*. JPL D-9930, California Inst. Technol., July 1992.
3. Lawrence, Roland W.; Bailey, M. C.; Harrington, Richard F.; Hearn, Chase P.; Wells, John; and Stanley, William D.: *Design and Development of a Multibeam 1.4 GHz Pushbroom Microwave Radiometer*. NASA TM-89005, 1986.
4. Special Issue on the Defense Meteorological Satellite Program (DMSP): Calibration and Validation of the Special Sensor Microwave/Imager (SSM/I). *IEEE Trans. Geosc. & Remote Sensing*, vol. 28, no. 5, Sept. 1990.
5. Menard, Y.; and Reynolds, M.: The Design of the ESA Multiband Imaging Microwave Radiometer MIMR. *Proceedings of the 11th Annual International Geoscience and Remote Sensing Symposium*, Volume 4, IEEE, 1991, pp. 2359–2363.
6. Tachi, Kazuo; Arai, Kohei; and Sato, Yuzi: Advanced Microwave Scanning Radiometer (AMSR): Requirements and Preliminary Design Study. *IEEE Trans. Geosc. & Remote Sensing*, vol. 27, no. 2, Mar. 1989, pp. 177–183.
7. Simpson, Joanne; Adler, Robert F.; and North, Gerald R.: A Proposed Tropical Rainfall Measuring Mission (TRMM) Satellite. *American Meteorol. Soc. Bul.*, vol. 69, Mar. 1988, pp. 278–295.
8. Rogers, Craig A.; and Stutzman, Warren L.: *Large Deployable Antenna Program—Phase I: Technology Assessment and Mission Architecture*. NASA CR-4410, 1991.
9. Kaminskas, Rimvydas A.: Stowable Reflector. U.S. Patent 4,811,034, Mar. 7, 1989.
10. Friesse, G.: *Inflated Concepts for the Earth Science Geostationary Platform and an Associated Flight Experiment*. NASA CR-187580, 1992.
11. Freeland, R. E.; Bilyeu, G. D.; and Veal, G. R.: *Validation of a Unique Concept for a Low-Cost, Lightweight Space-Deployable Antenna Structure*. IAF-93-I.1.204, Oct. 1993.
12. Kelleher, Kenneth S.; and Hyde, Geoffrey: Reflector Antennas. *Antenna Engineering Handbook*. Second Ed., Richard C. Johnson and Henry Jasik, eds., McGraw-Hill Book Co., 1984, pp. 17-1–17-41.
13. Nesti, Giuseppe: Long Term Stability Test on Two Plessey 90 GHz Noise Sources. *Microwave Radiometry and Remote Sensing Applications*, P. Pampaloni, ed., VSP BV (Zeist, The Netherlands), 1989, pp. 341–350.
14. Croswell, William F.; and Bailey, M. C.: Radiometer Antennas. *Antenna Engineering Handbook*. Second Ed., Richard C. Johnson and Henry Jasik, eds., McGraw-Hill Book Co., 1984, pp. 31-2–31-16.
15. Isakowitz, Steven J.: *International Reference Guide to Space Launch Systems—1991 Edition*. AIAA, 1991.
16. TRW To Build-Up to 12 Lightsats; First Launch Planned for 1992. *Avi. Week & Space Technol.*, vol. 132, no. 17, Apr. 23, 1990, pp. 24–25.

Table I. Ice Imaging Radiometer Characteristics

Instrument type . . . . .	Multiplexed conical pushbroom
Radiometer type . . . . .	Noise injection Dicke radiometer
Antenna . . . . .	4.3- by 8.2-m parabolic torus
Feed . . . . .	Printed circuit array
Polarization . . . . .	Dual linear (H and V)
Incidence angle, deg . . . . .	53
Frequency, GHz . . . . .	18.7 and 36.5
Footprint size, km . . . . .	5 and 2.5
Number of beams . . . . .	40 and 80
Number of radiometers . . . . .	10 and 20
Orbit altitude, km . . . . .	400
Swath width, km . . . . .	200
Revisit time, days . . . . .	3–5
Instrument power, W . . . . .	275
Instrument weight for—	
4- by 8-m faceted reflector, kg . . . . .	92
0.2- by 1-m feed panel with integrated radiometers, kg . . . . .	92
Ancillary equipment weight for—	
Telescoping mast, kg . . . . .	32
Small satellite bus (Eagle class), kg . . . . .	114
Solar cells, kg . . . . .	20
Reboost fuel (estimated), kg . . . . .	250
Total weight, kg . . . . .	600

Table II. Inflatable Antenna Radiometer Characteristics

Instrument type . . . . .	Multiplexed conical pushbroom
Radiometer type . . . . .	Noise injection Dicke radiometer
Antenna . . . . .	27- by 36-m parabolic torus
Feed . . . . .	Printed circuit array
Polarization . . . . .	Dual linear (H and V)
Incidence angle, deg . . . . .	53
Frequency, GHz . . . . .	1.413, 4.3, and 10.65
Footprint size, km . . . . .	10, 3.3, and 1.3
Number of beams . . . . .	16, 48, and 128
Number of radiometers . . . . .	4, 12, and 32
Orbit altitude, km . . . . .	400
Swath width, km . . . . .	160
Instrument power, W . . . . .	≈400
Instrument weight for—	
Inflatable antenna system, kg . . . . .	211
Feed assembly, kg . . . . .	183
Radiometer assembly, kg . . . . .	48
Cabling, kg . . . . .	18
Total instrument weight, kg . . . . .	460

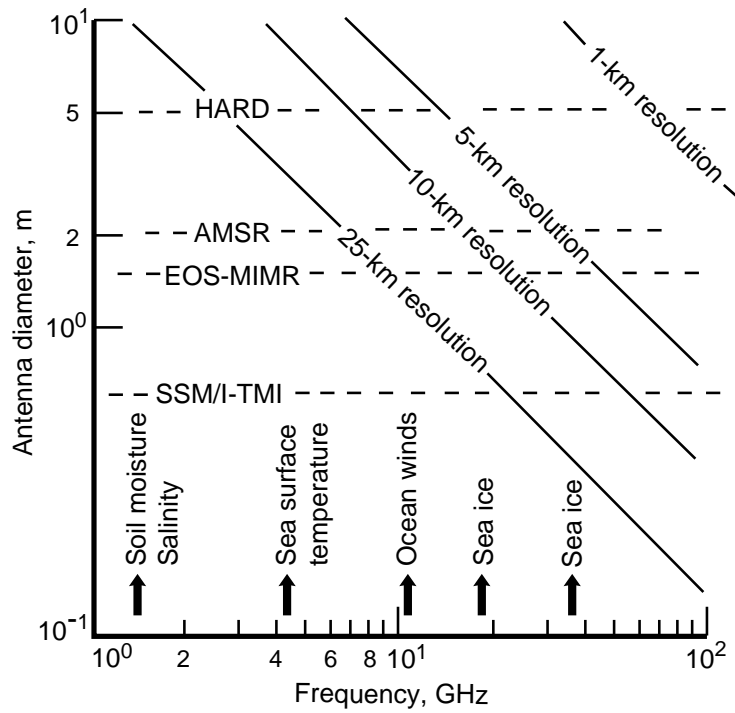


Figure 1. Required antenna diameter versus frequency for pushbroom radiometer at altitude of 400 km and incidence angle of  $50^\circ$ . Typical sensor frequencies and current space radiometer systems are shown.

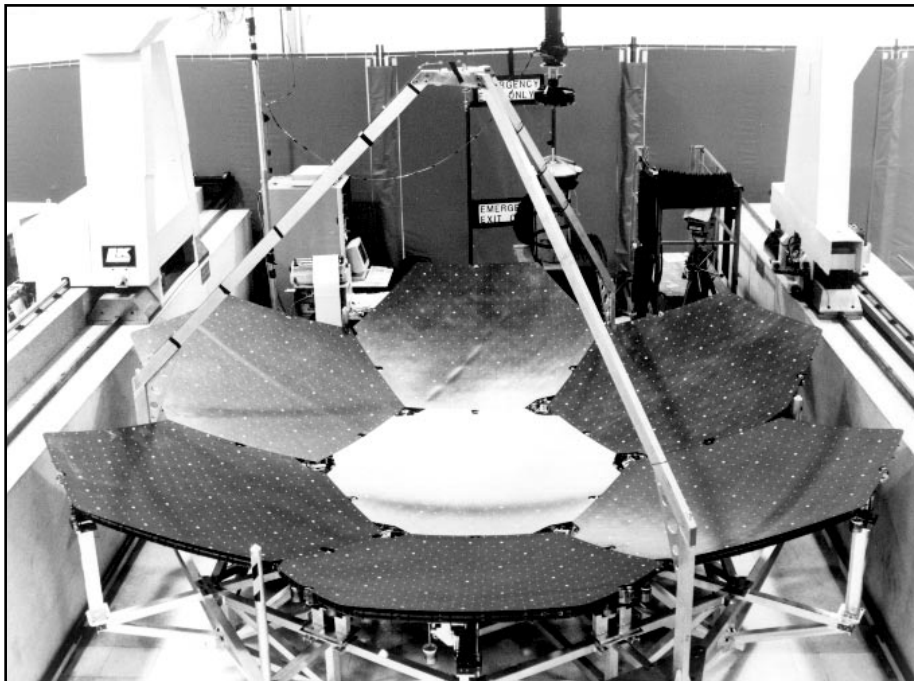


Figure 2. High accuracy reflector development (HARD) system, lightweight 5-m-diameter deployable prototype model.

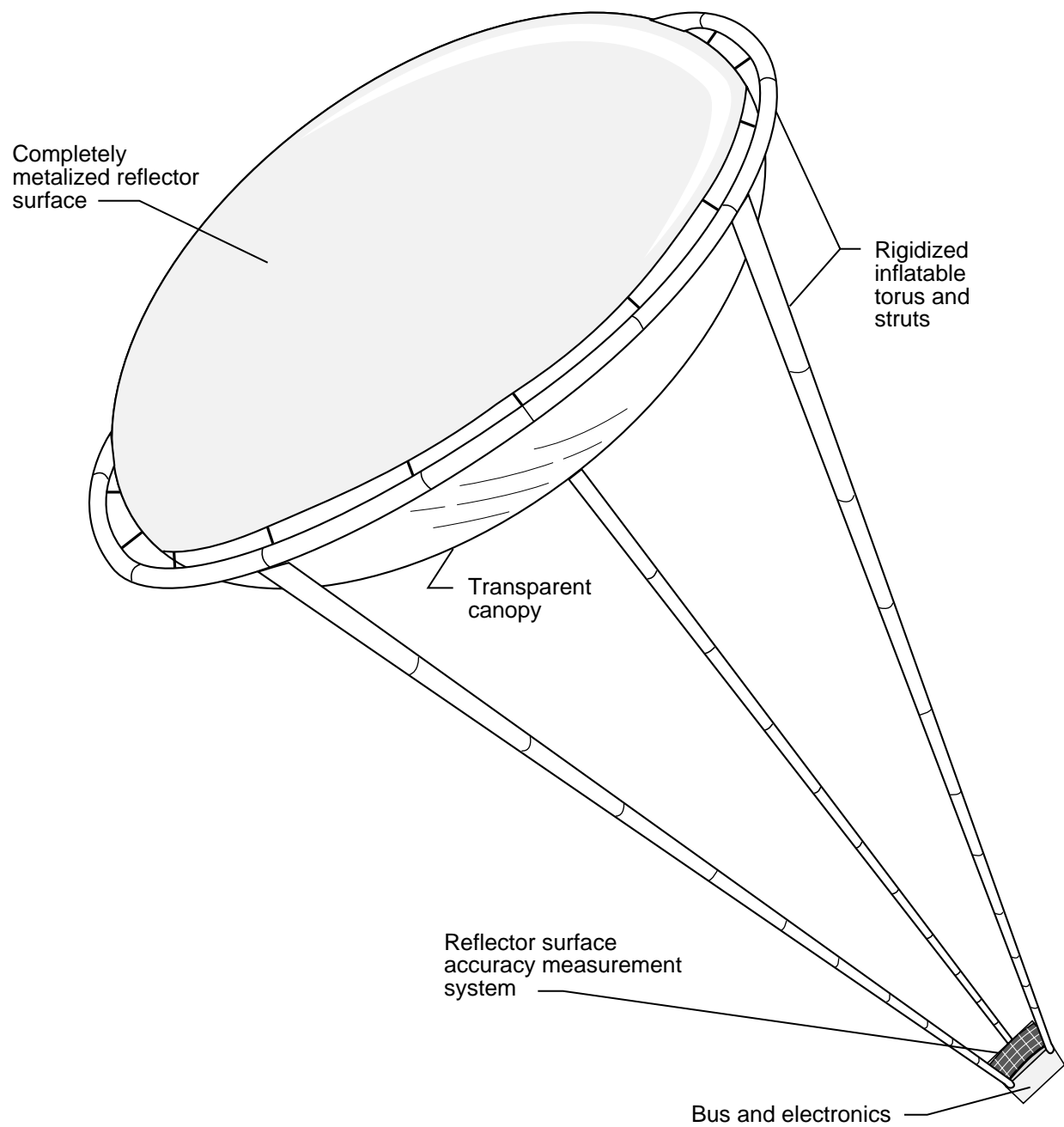


Figure 3. Inflatable 14.7-m-diameter antenna system being developed for IN-STEP program.



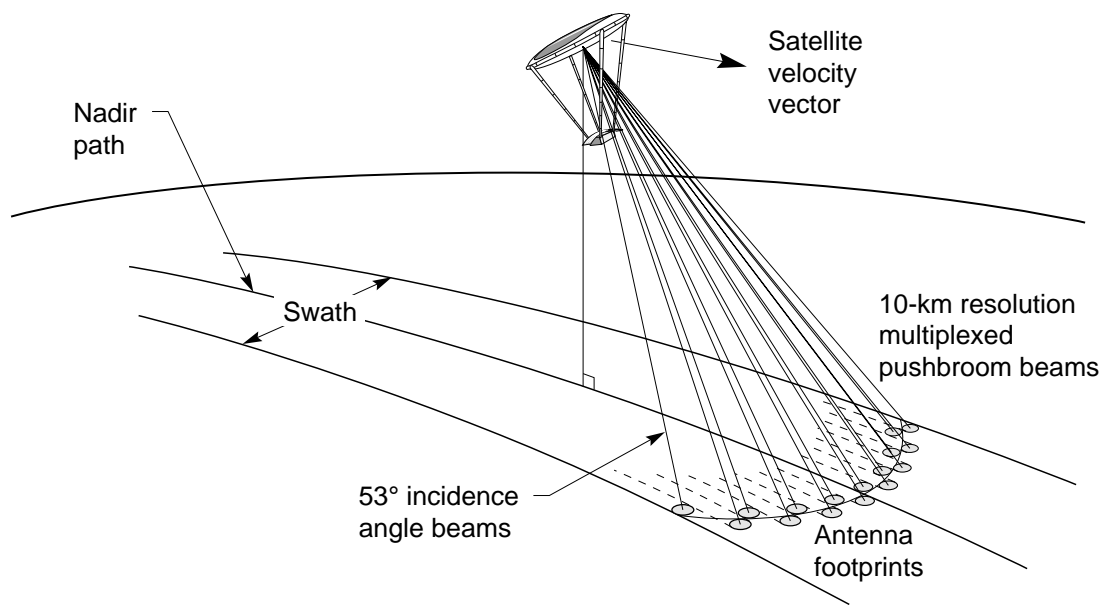


Figure 4. Conical pushbroom radiometer sensor.

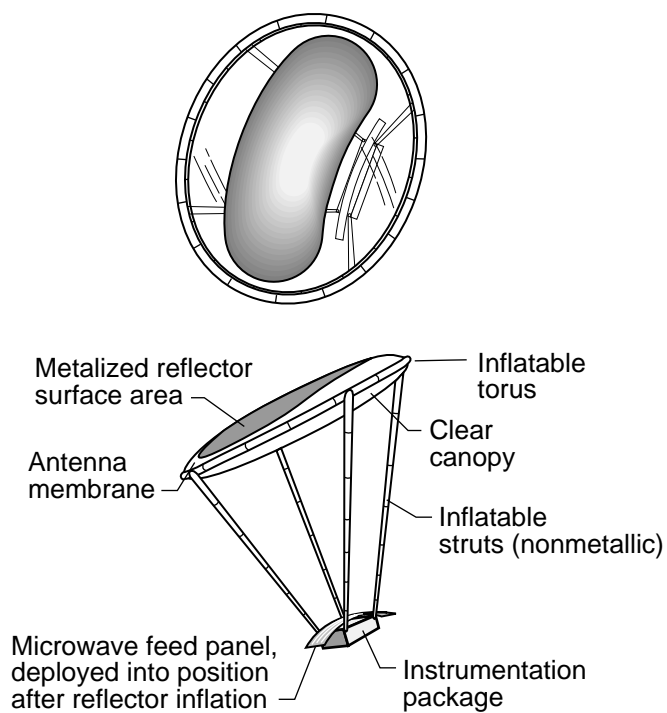


Figure 5. Soil moisture and oceanographic radiometer using inflatable reflector technology.

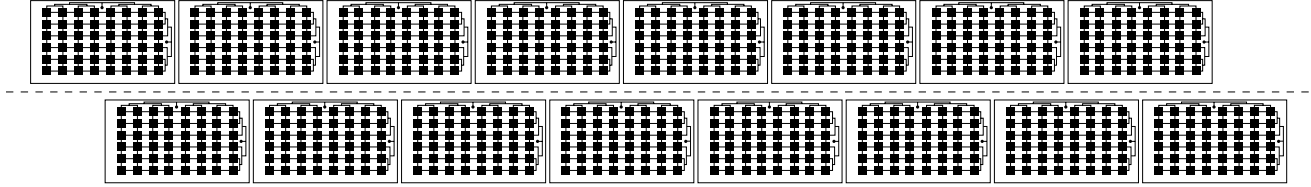


Figure 6. Feed panel for single-frequency pushbroom radiometer (16 beams).

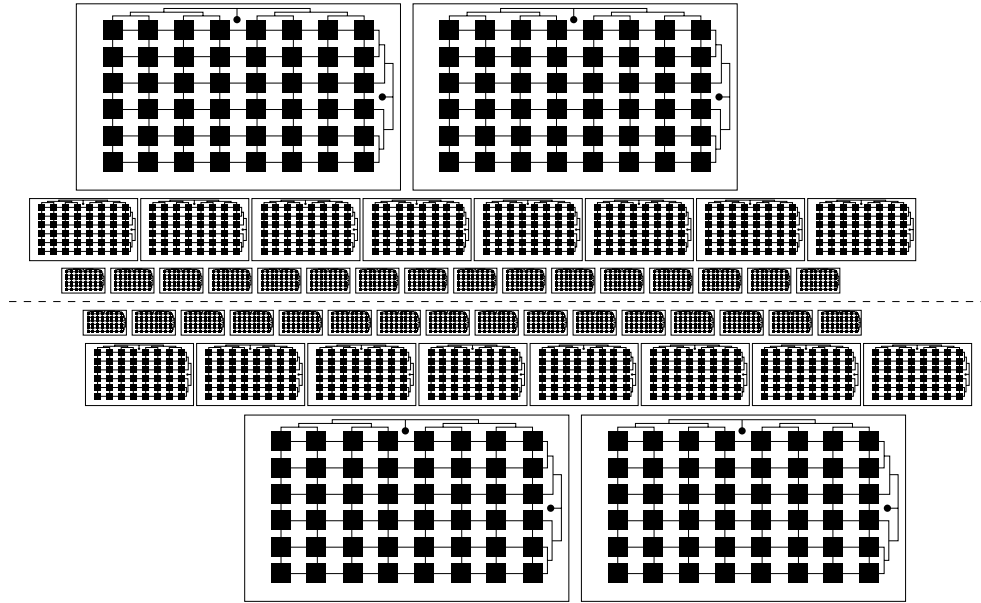


Figure 7. Feed panel for three-frequency pushbroom radiometer.

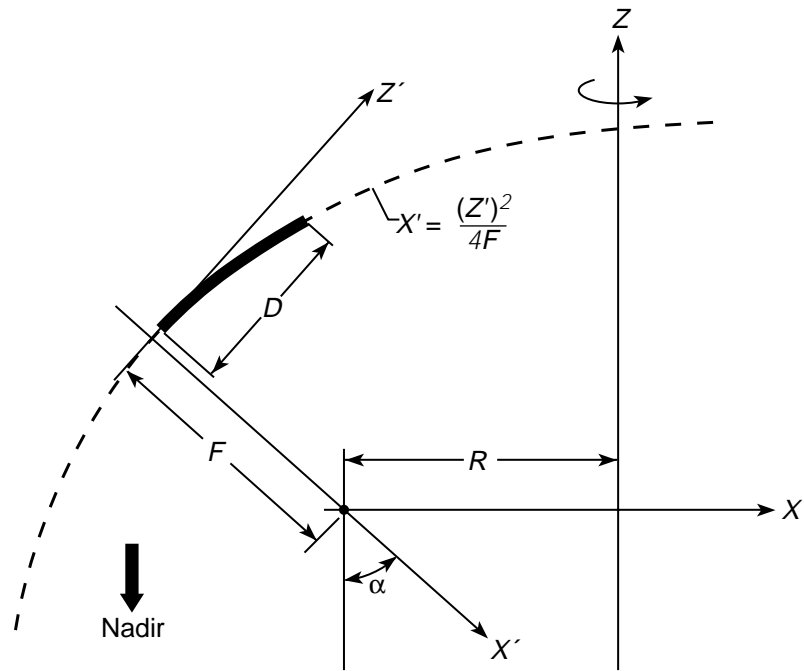


Figure 8. Geometry for parabolic torus reflector surface.

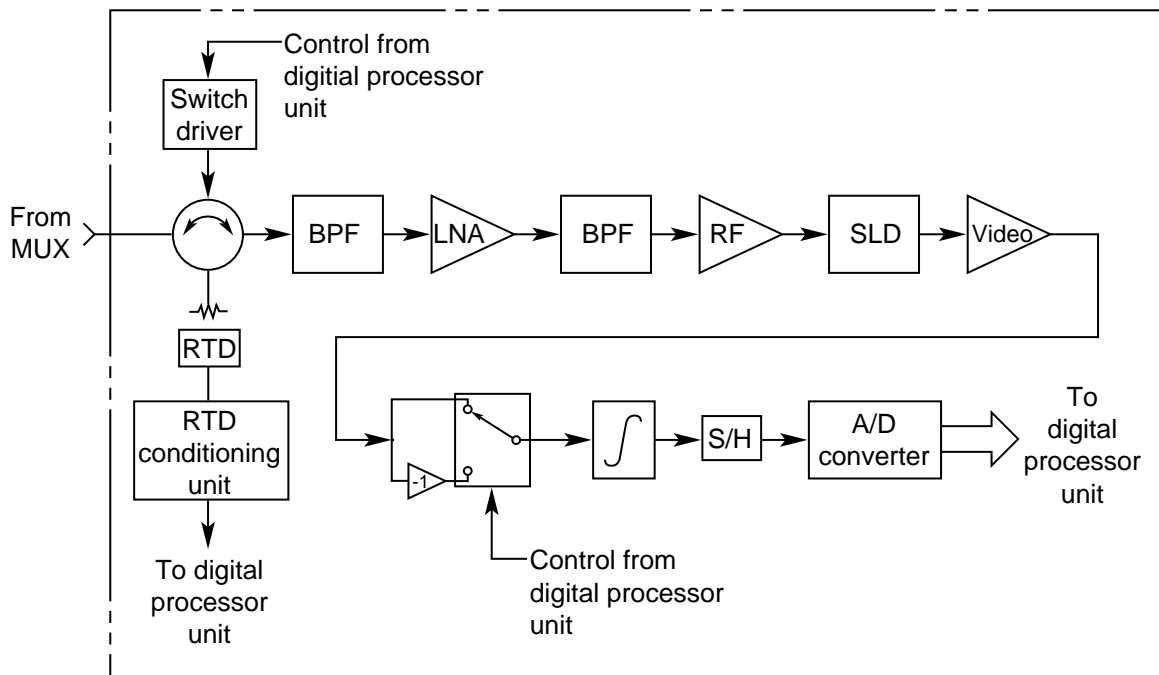


Figure 9. Radiometer receiver.

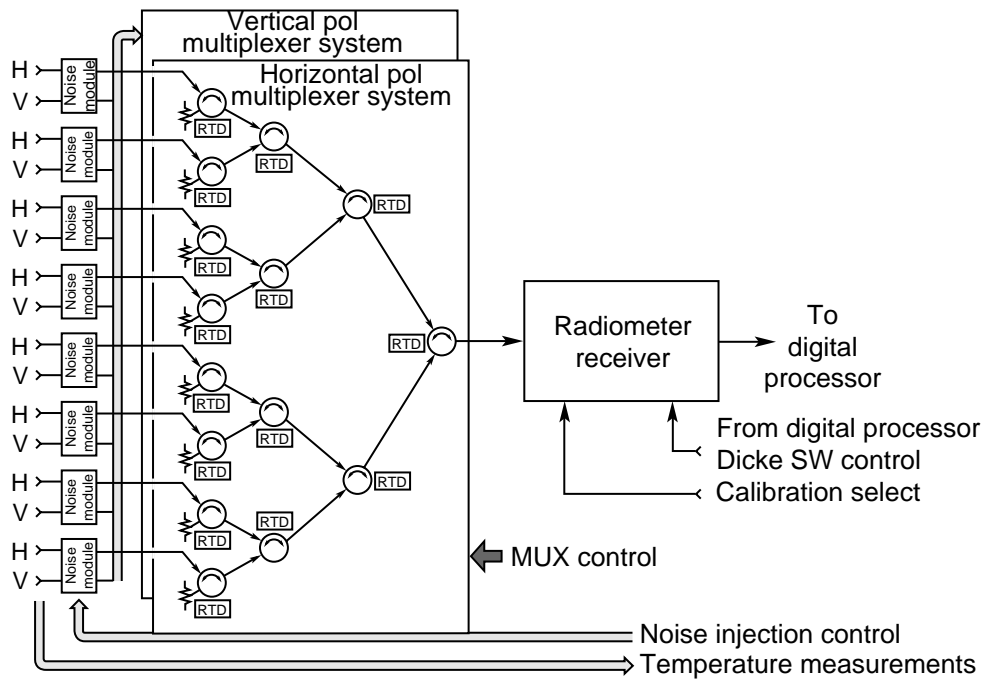


Figure 10. Radiometer assembly.

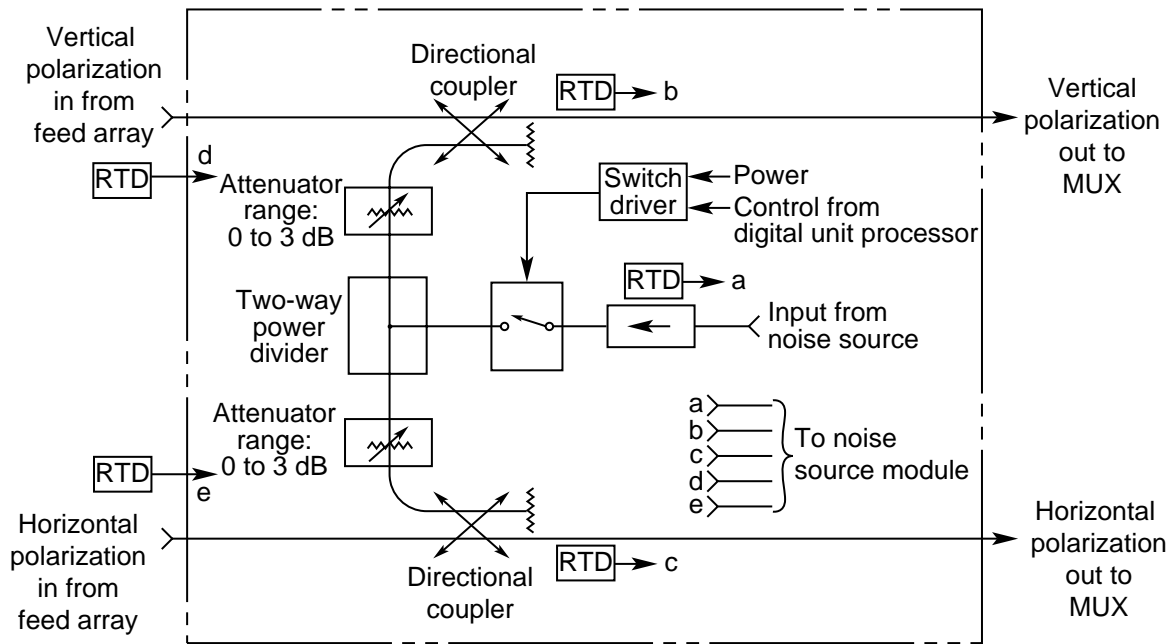


Figure 11. Radiometer noise module.

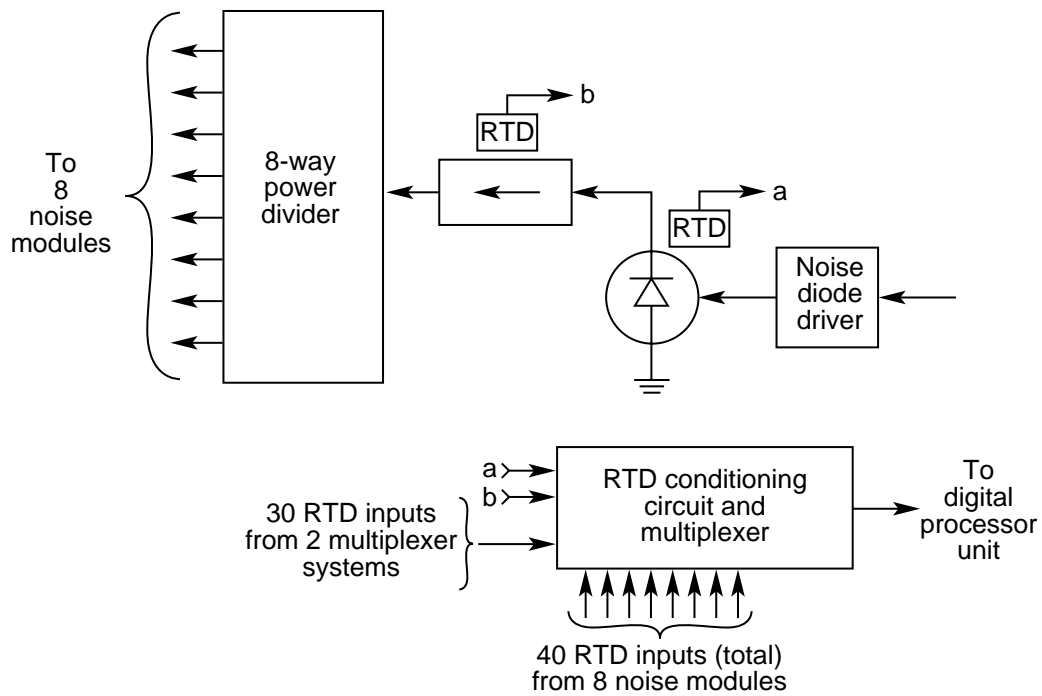


Figure 12. Radiometer noise source module.

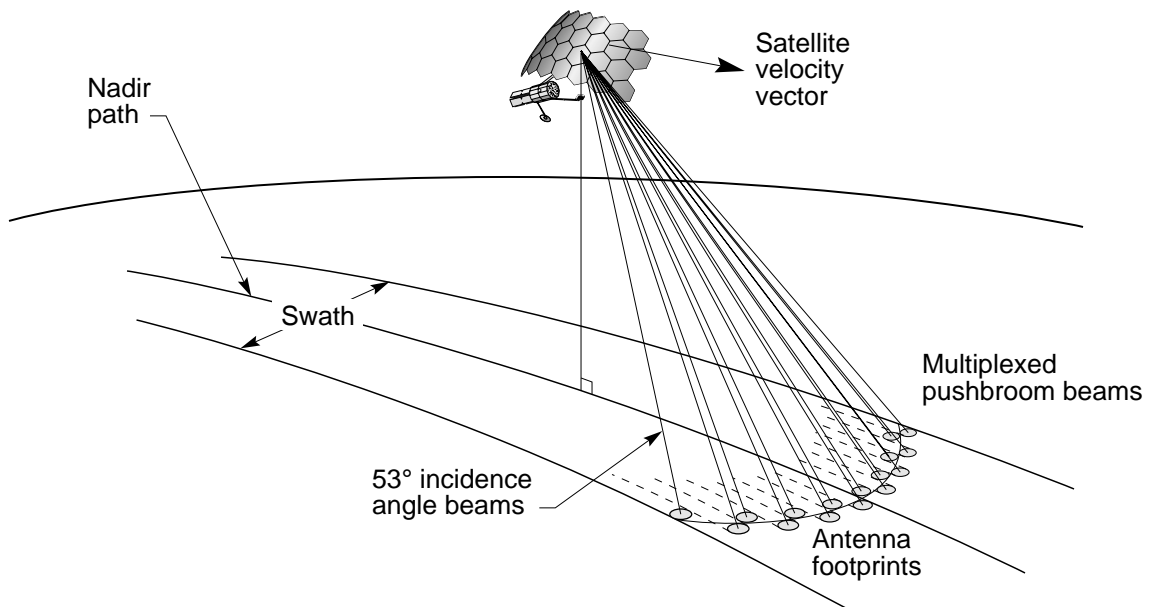


Figure 13. Multiplexed conical pushbroom ice imager.

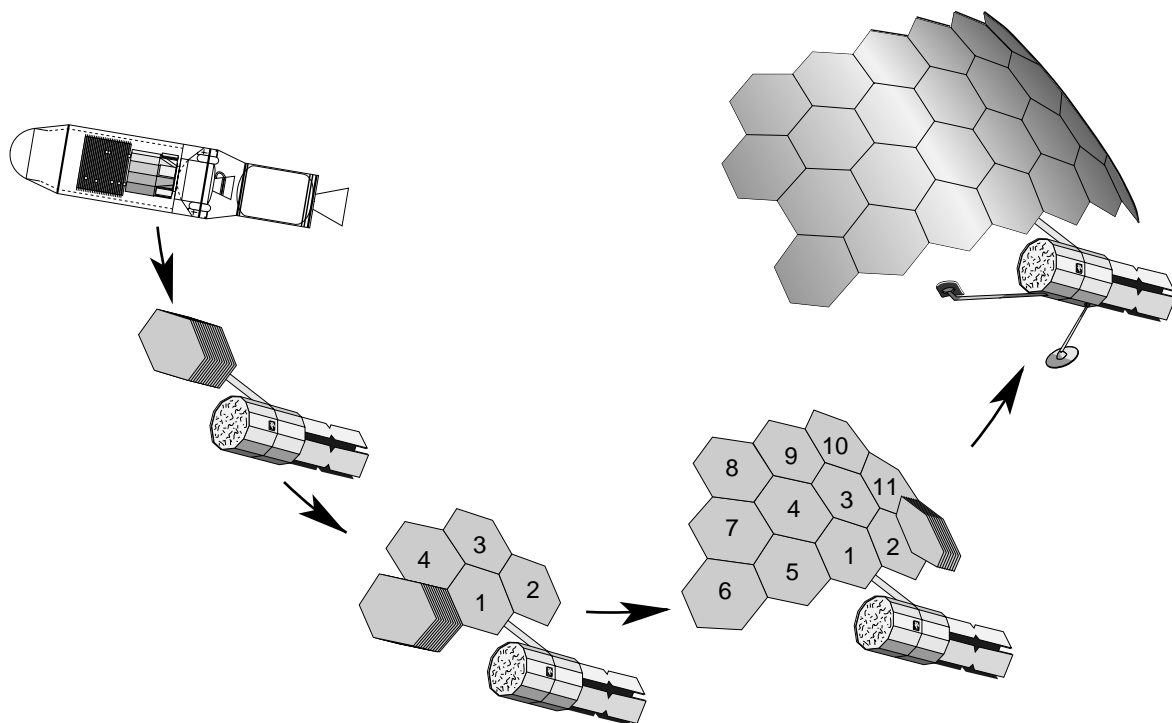


Figure 14. Deployment scenario for ice imaging radiometer system.

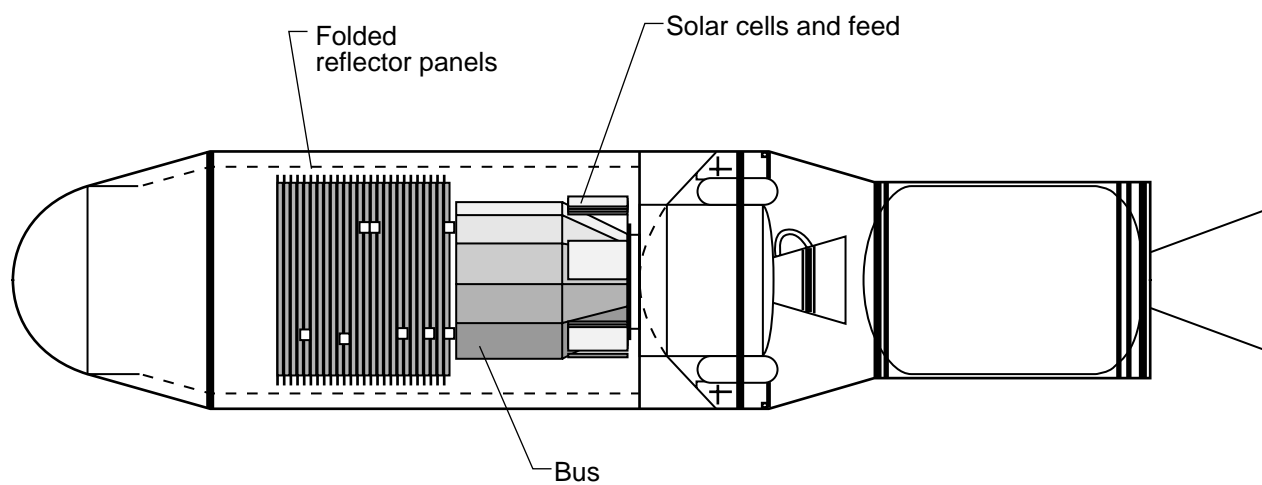


Figure 15. Launch packaging of HARD reflector and support systems on Taurus vehicle.

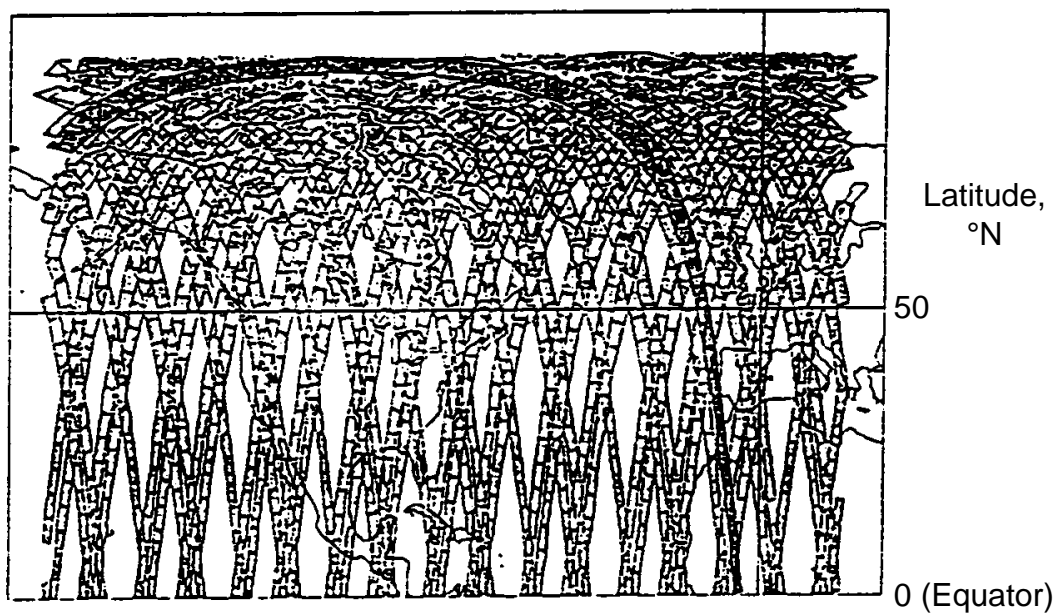


Figure 16. Coverage analysis summary for 3.54-day revisit time. Assumptions: altitude, 400 km; sun synchronous; inclination,  $97.07^\circ$ .

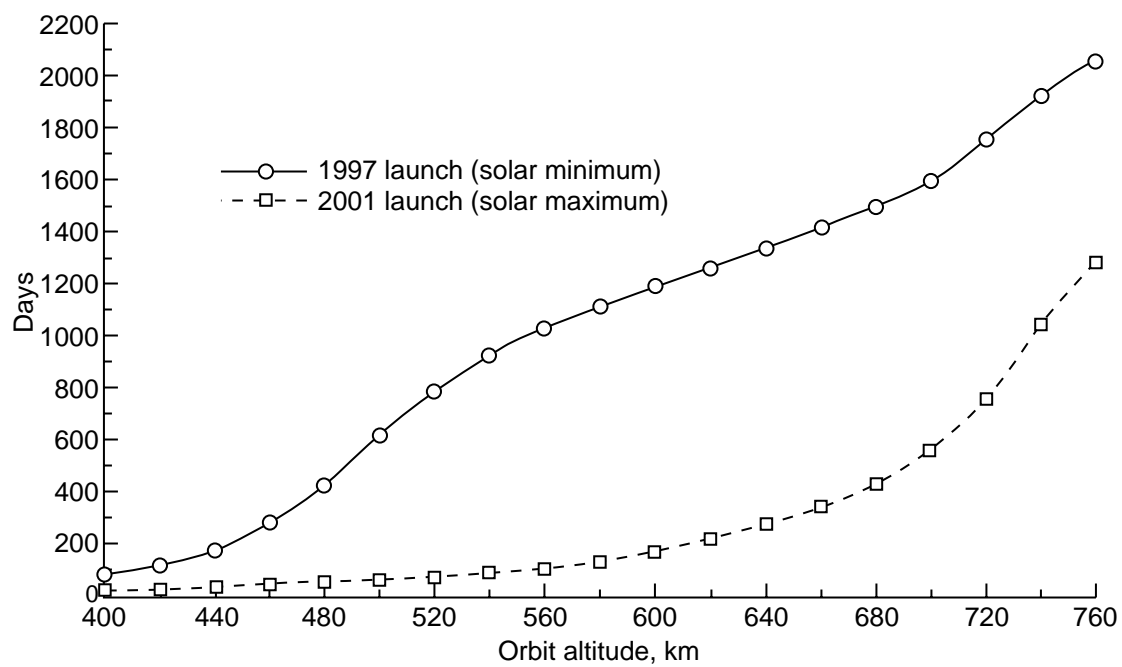


Figure 17. Orbit lifetime. Assumptions:  $2\sigma$  atmospheric model; 0,0,0 attitude with  $7.1 \text{ kg/m}^2$  ballistic coefficient.

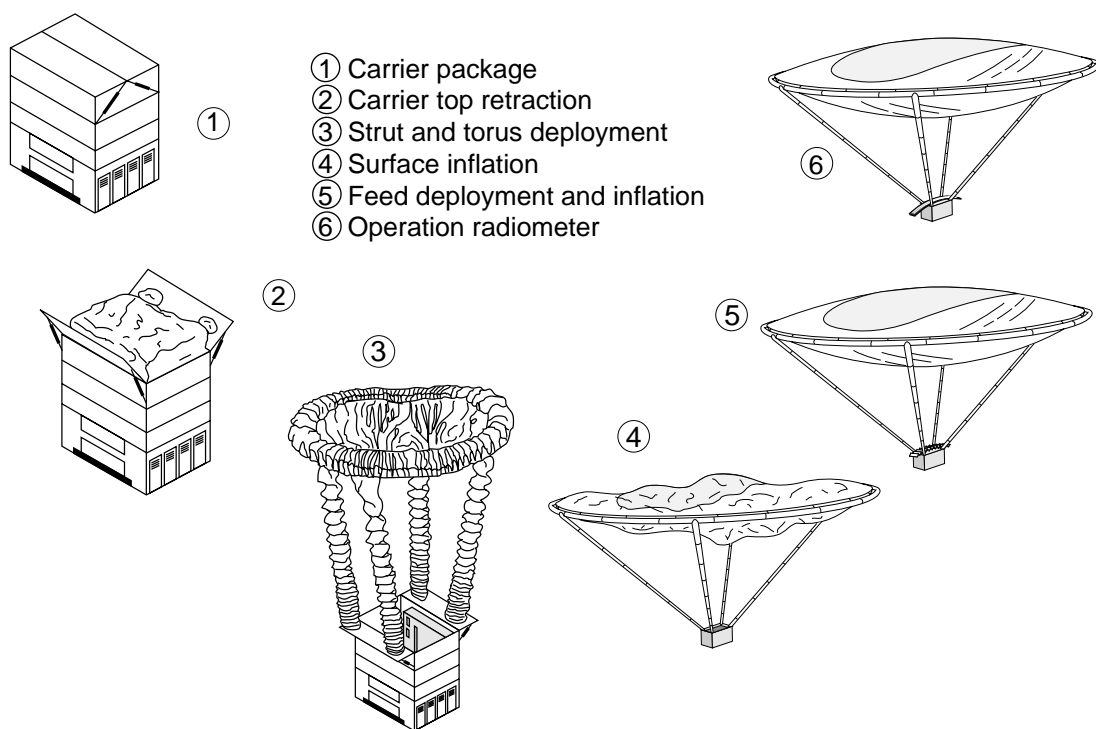


Figure 18. Deployment scenario for inflatable radiometer system.



<b>REPORT DOCUMENTATION PAGE</b>			Form Approved OMB No. 0704-0188	
Public reporting burden for this collection of information is estimated to average 1 hour per response, including the time for reviewing instructions, searching existing data sources, gathering and maintaining the data needed, and completing and reviewing the collection of information. Send comments regarding this burden estimate or any other aspect of this collection of information, including suggestions for reducing this burden, to Washington Headquarters Services, Directorate for Information Operations and Reports, 1215 Jefferson Davis Highway, Suite 1204, Arlington, VA 22202-4302, and to the Office of Management and Budget, Paperwork Reduction Project (0704-0188), Washington, DC 20503.				
<b>1. AGENCY USE ONLY (Leave blank)</b>		<b>2. REPORT DATE</b> September 1994	<b>3. REPORT TYPE AND DATES COVERED</b> Technical Paper	
<b>4. TITLE AND SUBTITLE</b> Design Studies of Large Aperture, High-Resolution Earth Science Microwave Radiometers Compatible With Small Launch Vehicles			<b>5. FUNDING NUMBERS</b>  WU 506-59-64-01	
<b>6. AUTHOR(S)</b> Lyle C. Schroeder, M. C. Bailey, Richard F. Harrington, Bruce M. Kendall, and Thomas G. Campbell				
<b>7. PERFORMING ORGANIZATION NAME(S) AND ADDRESS(ES)</b> NASA Langley Research Center Hampton, VA 23681-0001			<b>8. PERFORMING ORGANIZATION REPORT NUMBER</b>  L-17359	
<b>9. SPONSORING/MONITORING AGENCY NAME(S) AND ADDRESS(ES)</b> National Aeronautics and Space Administration Washington, DC 20546-0001			<b>10. SPONSORING/MONITORING AGENCY REPORT NUMBER</b> NASA TP-3469	
<b>11. SUPPLEMENTARY NOTES</b> Schroeder, Bailey, Kendall, and Campbell: Langley Research Center, Hampton, VA; Harrington: Old Dominion University, Norfolk, VA.				
<b>12a. DISTRIBUTION/AVAILABILITY STATEMENT</b>  Unclassified-Unlimited  Subject Category 43			<b>12b. DISTRIBUTION CODE</b>	
<b>13. ABSTRACT (Maximum 200 words)</b> High-spatial-resolution microwave radiometer sensing from space with reasonable swath widths and revisit times favor large aperture systems. However, with traditional precision antenna design, the size and weight requirements for such systems are in conflict with the need to emphasize small launch vehicles. This paper describes trade-offs between the science requirements, basic operational parameters, and expected sensor performance for selected satellite radiometer concepts utilizing novel lightweight compactly packaged real apertures. Antenna, feed and radiometer subsystem design and calibration are presented. Preliminary results show that novel lightweight real aperture coupled with state-of-the-art radiometer designs are compatible with small launch systems, and hold promise for high-resolution Earth science measurements of sea ice, precipitation, soil moisture, sea surface temperature, and ocean wind speeds.				
<b>14. SUBJECT TERMS</b> Large aperture antennas; Inflatable concepts; Lightweight facets; Pushbroom radiometer; Small launch vehicles			<b>15. NUMBER OF PAGES</b> 22	
			<b>16. PRICE CODE</b> A03	
<b>17. SECURITY CLASSIFICATION OF REPORT</b> Unclassified	<b>18. SECURITY CLASSIFICATION OF THIS PAGE</b> Unclassified	<b>19. SECURITY CLASSIFICATION OF ABSTRACT</b> Unclassified	<b>20. LIMITATION OF ABSTRACT</b>	